Pergamon

*Mechatronics* Vol. 5, No. 4, pp. 349–364, 1995

0957-4158/95 $9.50+0.00

0957–4158 (95) 00016-X

# SENSORLESS VELOCITY CONTROL FOR THE SERIES CONNECTED WOUND STATOR D.C. MOTOR

**T. BURG, D. DAWSON and P. VEDAGARBHA**

Department of Electrical and Computer Engineering, Clemson University, Clemson, SC 29634-0915, U.S.A.

(*Received* 19 *October* 1994; *accepted* 11 *January* 1995)

**Abstract**—A controller is designed to produce velocity trajectory following in a wound stator D.C. electric motor wired in a series configuration without the need for measurements of the mechanical states (i.e. *sensorless* control). The work represents a modification of a previously designed controller for the separately excited D.C. motor to address the more complicated problem of controlling the series connected motor. That is, a previous controller, which was designed in the framework of the *observed integrator backstepping* technique, is modified to reflect the peculiarities of the series connected motor dynamics. These modifications preclude a rigorous stability result; however, the control is validated through the use of a velocity tracking experiment on a commercial motor.

## 1. INTRODUCTION

The wound stator D.C. motor features a stator coil used to establish a magnetic field within the motor. A second wound coil, the rotor coil, directs a current to interact with the magnetic field in order to produce torque on the rotor coil and thus mechanical rotation of the rotor. Different speed and torque characteristics can be produced by connecting the two coils in a series, shunt, or separately excited manner to the electrical supply(s). It is the series connected configuration, where both coils experience the same current, that is considered in this paper. The series wound D.C. motor is often chosen for traction applications, such as subway trains, where its high start torque at low speeds distinguishes it from other D.C. motors [1].

There are three hurdles that make the series connection of the stator and rotor coils challenging from a sensorless control perspective. First, the torque applied to the rotor is a nonlinear positive function of the current in the coils. This implies that regardless of the sign of the input voltage, and hence the sign of the current, the motor can only produce a torque in one direction. Therefore, in designing a control for velocity trajectory tracking, the motor produced torque can only be used for acceleration; hence, the load torque and dampening forces must be used for deceleration. This will obviously limit the rate of deceleration and therefore the desired velocity trajectory must be chosen consistent with the load torque and the dampening forces. Second, the relationship between torque and current is complicated by the saturation effects in the stator magnetic circuit. Although this nonlinear relationship is often approximated by a linear model, we include this nonlinear effect in our control formulation. Third, certain operating conditions prevent observation of the rotor velocity from electrical measurements. Thus there must be some mechanism

included in the observer/controller that prevents disruption of the observer/controller in the region of these conditions or it must be shown that these conditions will not occur. The concept of applying nonlinear control techniques to a wound stator D.C. motor is well established. Use of more traditional nonlinear control techniques can be seen in the sliding mode controllers in [2] and [3] or the adaptive controller in [4]. In another approach [5] to this control problem, feedback linearization was used to design the nonlinear portion of the control which then rendered the remaining system amenable to standard linear control techniques. One of the most advanced systems for controlling the D.C. motor appears to be a feedback linearizing control used with a velocity observer for the series connected D.C. motor in [1] and the shunt connected D.C. motor in [6].

In addition to the above work, there has been much recent interest in the design of nonlinear controllers for mechanical systems actuated by electrical motors. For example, nonlinear controllers for the switched reluctance motor, permanent magnet stepper motor, brushless D.C. motor, and the induction motor were presented in [7–15]. All of this work has been directed at solving the position and/or velocity tracking control problem with measurement of position and/or velocity and some or all of the electrical states. Since the instrumentation used to measure the motion of the mechanical system is in general more costly than the devices used to measure electrical states such as current, it would be desirable to eliminate the need for the more costly mechanical system sensors. Many recent research papers [16, 17] use the terminology *sensorless* control to describe a control approach which eliminates the use of mechanical system sensors; however, many of the proposed techniques are based on a simplified set of static equations rather than the dynamic equations which govern the motion of the electromechanical system.

In [18], a controller was designed to produce velocity trajectory following in a separately excited wound stator D.C. motor. The separately excited configuration provides the designer with two voltage inputs to the motor, namely the stator and rotor voltages. This controller was formulated for the two control inputs using the observed integrator backstepping [19] nonlinear control design technique. The result was an observer and controller which yielded exponential velocity tracking provided the stator current was not equal to *zero*. Since the stator coil can be controlled independently from the rotor coil, the stator control voltage was designed to drive the stator current to a positive constant, thus minimizing the possibility of *zero* stator current. The rotor voltage was then used to servo the rotor velocity. The extension of this work to the series connection is complicated by the fact the stator and rotor coils experience the same current. We cannot therefore isolate the need to prevent *zero* stator current from the requirement of servoing the rotor velocity. However, the basic design methodology presented in [18] can be modified to design a velocity controller for the series connected motor. Unfortunately, the cost of combining the objectives of the two control inputs into a single control input is the loss of a general statement on stability; however, experimental results illustrate that the design procedure leads to a working controller in spite of the loss of the stability guarantee.

This paper is organized to illustrate the design of the sensorless velocity controller. The starting point of the design is the electromechanical model of the motor presented in section 2. Based on this electromechanical model, a nonlinear first-order observer is designed in section 3. The velocity observer is then accounted for during

the nonlinear input voltage controller designed in section 4. The paper culminates with a demonstration of the proposed controller in a velocity tracking experiment described in section 5.

## 2. PROBLEM STATEMENT

### *2.1. System model of a series connected D.C. motor*

Viewed as a "black box", the dynamic model of the series connected D.C. motor has one input and one output, the motor terminal voltage and the rotor velocity, respectively. This "black box" behavior can be decomposed into a set of cascaded dynamic subsystems for the purpose of controller design. The mechanical subsystem dynamics of the series connected D.C. motor [1] are given by

$$M\dot{\omega} + B\omega + T_L = \tau, \tag{1}$$

where $\omega(t)$ is the velocity of the rotor shaft, the constant mechanical parameter $M$ specifies the combined inertia of the rotor and the connected load, the constant mechanical parameter $B$ relates the effects of viscous friction in the system, and $\tau(t)$ is the motor torque. Additionally, the term $T_L$ represents a constant external force applied to the rotor as a result of the connected load.

The algebraic torque production equation

$$\tau = K_\tau g(I)I \tag{2}$$

quantifies the "motor action" in that it relates the amount of torque appearing on the rotor to the amount of current in the rotor coil, $I(t)$, and the magnitude of the magnetic flux, $g(I(t))$, produced by the stator coil. The constant torque transmission parameter, $K_\tau$, is a function of the motor construction. The function $g(I)$ is used to model the saturation effect in the stator magnetic circuit; i.e. increases in the stator current have a diminishing effect on torque production. The form of $g(I)$ is constrained for the controller developed here by: (i) $g(0) = 0$ and (ii) $g(I)$ is a strictly increasing, differentiable function. Often the function $g(I)$ is approximated by a linear model, i.e. $g(I) = L_S I$, where $L_S$ is the constant inductance of the stator.

In the series connection of the wound stator D.C. motor, the input voltage will appear across the series connection of the rotor and stator coils; therefore, the stator and rotor coils will experience the same current. It will be assumed in the model presented here that

$$\frac{\partial}{\partial I}[g(I)] \gg L_R,$$

where $L_R$ is the constant rotor inductance [1]. The dynamic relationship between the coil current and the input motor voltage, $v(t)$, is contained in the electrical subsystem as [1]

$$\frac{\partial}{\partial I}[g(I)]\dot{I} + RI + K_B\omega g(I) = v. \tag{3}$$

The electrical parameters $R$ and $K_B$ specify the combined constant resistances of the rotor and stator coils and the back-emf voltage constant, respectively. Note that this model for the series connected motor assumes no field weakening, i.e. the armature and field coils experience the same current.

**Remark 2.1.** It should be noted from Eqn (2) and the assumed form of $g(I)$ that the developed motor torque is positive regardless of the sign of the current and therefore the electric current can only be used to accelerate the motor.

**Remark 2.2.** The form of the electrical dynamics in Eqn (3) suggests the possibility of observing the rotor velocity from electrical measurements (this possibility was brought to our attention in [1]), i.e. Eqn (3) can be arranged such that the velocity $\omega$ is explicitly written in terms of $I$, $\dot{I}$, and $v$. Unfortunately, this arrangement will require division by $g(I)$ and will therefore not allow for velocity estimation when $I = 0$. That is, the condition $I = 0$ does not correspond to a unique rotor velocity in this relationship and places a physical limitation on velocity estimation at this value of current. Later, when we exploit the structure of the back-emf term in Eqn (3) to develop an observer for the rotor velocity, we must be wary of the operating condition $I = 0$.

### *2.2. Control design objective*

The goal of this work is to design a voltage-level control input to the motor that will provide for tracking of a specified velocity trajectory. The controller design is predicated on exact model knowledge of the nonlinear differential equations in Eqns (1) through (3), i.e. these equations accurately reflect the dynamics of the motor to be controlled. The control signal will be generated from measurements of the winding current and estimates of the rotor velocity. The variation of the velocity estimate, $\hat{\omega}(t)$, from the true velocity is defined as

$$\tilde{\omega} = \omega - \hat{\omega}. \tag{4}$$

Since the true velocity will not be measured, tracking of the rotor velocity to the desired velocity, $\omega_d(t)$, will be inferred from the closeness of the observed rotor velocity, $\hat{\omega}(t)$, to the desired velocity. The velocity tracking error defined in this manner is quantified as

$$e = \omega_d - \hat{\omega}. \tag{5}$$

In the ensuing controller and observer developments, it will be required that the desired velocity is bounded and has bounded first and second derivatives.

## 3. VELOCITY OBSERVER DEVELOPMENT

The shaft velocity, $\omega(t)$, is estimated in order to circumvent the need for velocity measurements in the controller design. In this section we present the observer designed to produce such estimates and a description of the design process.

*3.1. Velocity observer*

The dynamic equation that will be implemented to observe the rotor velocity is given by

$$\hat{\omega} = z - \frac{k_0}{MK_B} f(I) \tag{6}$$

$$\dot{z} = M^{-1}\left(\frac{k_0}{K_B}\left(\frac{v - RI}{g(I)}\right) - k_0\hat{\omega} - B\hat{\omega} - T_L + K_\tau I g(I)\right), \tag{7}$$

where $\hat{\omega}(t)$ is the velocity estimate, $k_0$ is an arbitrary positive gain that will be used to modify the observer behavior, and $f(I)$ is a function which must be selected to satisfy to the following relationship:

$$\frac{\partial}{\partial I}[f(I)] = \frac{\frac{\partial}{\partial I}[g(I)]}{g(I)}. \tag{8}$$

The intermediate variable $z(t)$ is used to separate the observer into two implementable equations. That is, this same observer written in a single equation realization would require the measurement of $\omega(t)$ [see Eqn (13) below].

**Remark 3.1.** In order to implement the observer, we must preclude the possibility of division by *zero* in Eqns (7) and (8). To this end, we will replace the true current signal $I$ with $I_{\text{filt}}$ in the two instances where *zero* current will disrupt the observer. The positive filtered current signal, $I_{\text{filt}}$, is generated according to

$$I_{\text{filt}} = \begin{cases} I & \text{for } \alpha < I \\ \alpha & \text{elsewhere} \end{cases}, \tag{9}$$

where $\alpha$ is a small positive constant.

**Remark 3.2.** The structure of the above observer is very similar to the one presented by Chiasson [1] which was developed using differential-geometric techniques; however, the order has been reduced. Of particular significance is the fact that the solution to Eqn (8) was used as the change of coordinate transformation in [1].

*3.2. Velocity observer design*

To motivate the form of the observer given above we apply a Lyapunov-like approach to the velocity estimation error. That is, we will use the non-negative, scalar function $V_0(t)$ given by

$$V_0 = \tfrac{1}{2} M \tilde{\omega}^2 \tag{10}$$

with a time derivative given by

$$\dot{V}_0 = \tilde{\omega} M \dot{\tilde{\omega}}. \tag{11}$$

The observer design proceeds by postulating a crude observer as described in Remark 2.2 and then adding terms until it can be seen that $\dot{V}_0(t)$ is non-positive. In a typical Lyapunov analysis, these conditions on $V_0(t)$ and $\dot{V}_0(t)$ would be used to guarantee an exponentially stable observer; however, here we are only using this approach as a guide for the design procedure.

The Lyapunov-like analysis is demonstrated using the final form of the observer in Eqns (6), (7), and (8). First, Eqns (6), (7), and (8) are combined into a single equation. This operation is accomplished by differentiating Eqn (6), multiplying by $M$, and substituting for $\dot{z}$ from Eqn (7) and for $\partial[f(I)]/\partial I$ from Eqn (8) to produce a single realization of the velocity estimator as

$$M\dot{\hat{\omega}} = \frac{k_0}{K_B}\left(\frac{v - RI}{g(I)}\right) - k_0\hat{\omega} - B\hat{\omega} - T_L + K_T I g(I) - \frac{k_0}{K_B}\left(\frac{\dfrac{\partial}{\partial I}[g(I)]}{g(I)}\dot{I}\right). \quad (12)$$

The electrical subsystem dynamics in Eqn (3) are substituted for $\partial[g(I)]/\partial I\dot{I}$ in Eqn (12), and then through algebraic manipulation and use of the definition of $\tilde{\omega}$ in Eqn (4), the result simplifies to

$$M\dot{\hat{\omega}} = k_0\tilde{\omega} - B\hat{\omega} - T_L + K_T I g(I). \quad (13)$$

The term $M\dot{\omega}$ is subtracted from both sides of Eqn (13), the mechanical dynamics in Eqn (1) are substituted for $M\dot{\omega}$ on the resulting right-hand side, the definition of $\tau$ is substituted from Eqn (2), and finally the definition of $\tilde{\omega}$ is substituted into the resulting right-hand side to produce

$$M\dot{\tilde{\omega}} = -k_0\tilde{\omega} - B\tilde{\omega}. \quad (14)$$

The estimation error dynamics in Eqn (14) are now substituted into Eqn (11) to yield the fact that $\dot{V}_0$ is non-positive as shown by

$$\dot{V}_0 \leq -k_0\tilde{\omega}^2. \quad (15)$$

**Remark 3.3.** Although we are blocked from proceeding further with a global stability analysis by the fact that the condition $I = 0$ can disrupt the observer, we can look to the stability analysis for some suggestion as to how the observer will perform outside of this condition. The standard conclusion from Eqns (10) and (15) is that the estimation error will approach *zero* exponentially fast. Therefore, the observer will successfully estimate the rotor velocity provided that the condition $I = 0$ does not occur. The effects of the current filter in Remark 3.1, to prevent the condition $I = 0$ when the observer is implemented, cannot be predicted by the above analysis.

**Remark 3.4.** Equation (12) can be considered as the design equation for the observer. In Eqns (13) and (14), it can be seen that the observer has been specifically designed to achieve Eqn (15). The implementable observer in Eqns (6) and (7) is then obtained by working backwards from Eqn (12). The terms that need to be differentiated to achieve Eqn (12) are grouped in Eqn (6) while the terms that should appear directly in Eqn (12) are grouped in Eqn (7).

## 4. SENSORLESS VELOCITY CONTROL DEVELOPMENT

The voltage control input is now designed through a two step process suggested by the integrator backstepping technique [19]. First, a desired torque signal is proposed for the mechanical subsystem. This desired torque signal, if it could be directly applied to the mechanical subsystem, would produce the desired velocity trajectory following. However, looking back to the motor model we see that the input to the motor is the applied terminal voltage. Therefore in the second step a voltage input is designed to produce the desired torque signal as the output of the electrical subsystem. This design process mandates the use of the velocity estimate in the voltage control input.

### *4.1. Voltage input controller*

To achieve the desired velocity tracking, the following input control voltage, $v(t)$, is proposed:

$$v = \frac{1}{\Omega_4}(\Omega_1 + \Omega_2\hat{\omega} + k_s\eta + k_{N2}(\Omega_2 + \Omega_3)^2\eta + K_\tau e), \tag{16}$$

where the positive gains $k_s$ and $k_{N2}$ can be adjusted to improve the controller performance. The *measurable* auxiliary variables introduced in Eqn (16) are given by

$$\begin{aligned}
\Omega_1 &= \Omega_4 RI + \frac{M\dot{\omega}_d}{K_\tau} + \frac{B}{MK_\tau}(K_\tau Ig(I) - T_L - B\hat{\omega}) \\
&\quad + \frac{(k_s + k_{N1}k_0^2)}{MK_\tau}(M\dot{\omega}_d + B\hat{\omega} + T_L - K_\tau Ig(I)) \\
\Omega_2 &= \Omega_4 K_B g(I) \\
\Omega_3 &= \frac{k_0}{MK_\tau}(B - k_{N1}k_0^2 - k_s) \\
\Omega_4 &= I + \frac{g(I)}{\frac{\partial}{\partial I}[g(I)]},
\end{aligned} \tag{17}$$

where $k_{N1}$ is a positive constant gain. The voltage input of Eqn (16) includes a desired torque signal that is embedded in the torque tracking error $\eta(t)$ which is defined by

$$\eta = \tau_d - Ig(I), \tag{18}$$

where a small value of $\eta(t)$ implies that the desired torque signal is being output by the electrical subsystem. Based on the mechanical dynamics in Eqn (1), the desired torque signal

$$\tau_d = \frac{1}{K_\tau}(M\dot{\omega}_d + B\hat{\omega} + T_L + k_s e + k_{N1}k_0^2 e) \tag{19}$$

is proposed for velocity tracking in the mechanical subsystem. The desired torque signal includes previously introduced variables and the two positive constant gains, $k_s$ and $k_{N1}$, that can also be adjusted to improve the controller performance.

There are two conditions that may disrupt generation of the input control voltage. First, as was the case in the observer, we must guard against division by *zero* [see Eqn (16) for division by $\Omega_4$]. In practice this is achieved by using the filtered current signal, $I_{\text{filt}}$, to replace the mischievous occurrences of $I$ in the auxiliary variable $\Omega_4$ of Eqn (17) as follows:

$$\Omega_4 = I_{\text{filt}} + \frac{g(I_{\text{filt}})}{\dfrac{\partial}{\partial I}[g(I_{\text{filt}})]}.$$

Second, the signal $\tau_d(t)$ generated according to Eqn (19) is not guaranteed to conform to the positive-only torque producing capability of the motor. To avoid specifying an unachievable torque command, the signal $\tau_d(t)$ is replaced by the filtered torque signal $\tau_{d\text{filt}}$ that will be specified to conform to the positive-only torque producing capability. The filtered desired torque signal used for implementation of the controller is

$$\tau_{d\text{filt}} = \begin{cases} 0 & \text{for } \tau_d \leq 0 \\ \tau_d & \text{for } 0 < \tau_d \end{cases}.$$

A block diagram summarizing the proposed observer/controller system is shown in Fig. 1.

### 4.2. *Motivation for the controller structure*

The controller design is also guided by a Lyapunov-like analysis. The design is centered around the non-negative function

$$V = V_0 + \tfrac{1}{2}Me^2 + \tfrac{1}{2}\eta^2, \tag{20}$$

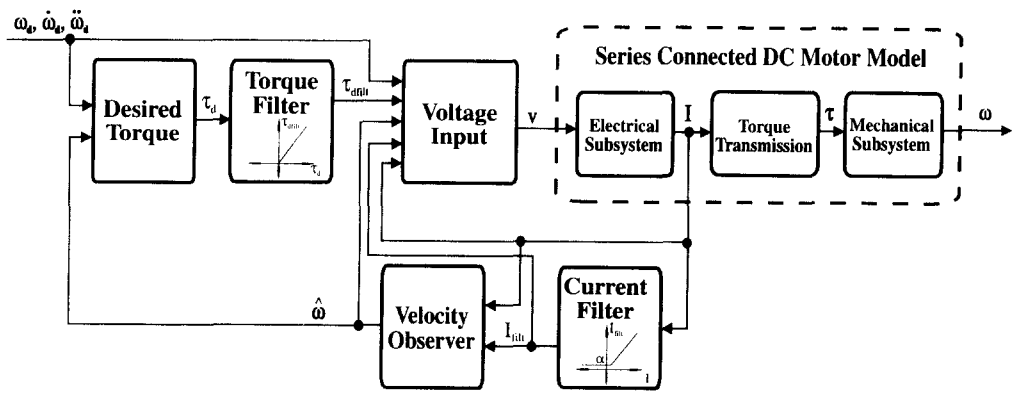


Fig. 1. Controller block diagram.

where $V_0(t)$ was defined in Eqn (10), and the first time derivative of $V(t)$ is given by

$$\dot{V} = \dot{V}_0 + M\dot{e}e + \dot{\eta}\eta. \tag{21}$$

The controller is designed by modifying a proposed input control voltage until it can be seen that $\dot{V}(t)$ is non-positive. This is an inherently iterative design process. The final iteration of the design is given below.

In order to show that $\dot{V}(t)$ in Eqn (21) is non-positive, we must substitute dynamic expressions for each of the derivative terms on the right-hand side of Eqn (21) formed from the observer and the electromechanical dynamics. The first term, $\dot{V}_0(t)$, was found in Eqn (15) and the two remaining terms are found as follows. The definition of $e$ in Eqn (5) is differentiated with respect to time and multiplied by $M$, and then a substitution is made for $M\dot{\hat{\omega}}$ from Eqn (13) to yield

$$M\dot{e} = M\dot{\omega}_d - k_0\tilde{\omega} + B\hat{\omega} + T_L - K_\tau Ig(I). \tag{22}$$

As the error dynamics in Eqn (22) lack a control input, the embedded control input, $\tau_d$, is injected into the error system by adding and subtracting $K_\tau\tau_d$ to the right-hand side of Eqn (22) to produce

$$M\dot{e} = M\dot{\omega}_d + B\hat{\omega} + T_L - k_0\tilde{\omega} - K_\tau\tau_d + K_\tau\eta, \tag{23}$$

where $\eta$ was defined in Eqn (18). The desired torque signal $\tau_d$ term can be substituted from Eqn (19) into Eqn (23) to yield the final form for the velocity tracking error dynamics

$$M\dot{e} = -k_s e - k_0\tilde{\omega} - k_{N1}k_0^2 e + K_\tau\eta. \tag{24}$$

The torque tracking error dynamics can be described by first differentiating the torque tracking error in Eqn (18) to yield

$$\dot{\eta} = \dot{\tau}_d - \dot{I}g(I) - I\frac{\partial}{\partial I}[g(I)]\dot{I}, \tag{25}$$

which can be written as

$$\dot{\eta} = \dot{\tau}_d - \dot{I}\left(g(I) + I\frac{\partial}{\partial I}[g(I)]\right). \tag{26}$$

The electrical subsystem dynamics in Eqn (3) can be solved for $\dot{I}$ and substituted into Eqn (26) to produce

$$\dot{\eta} = \dot{\tau}_d + (RI + K_B\omega g(I) - v)\left(\frac{g(I)}{\dfrac{\partial}{\partial I}[g(I)]} + I\right). \tag{27}$$

The definition of $\Omega_4$ in Eqn (17) is invoked to rewrite Eqn (27) as

$$\dot{\eta} = \dot{\tau}_d + RI\Omega_4 + K_B\omega g(I)\Omega_4 - \Omega_4 v. \tag{28}$$

The derivative of the desired torque control signal in Eqn (28) is found by differentiating Eqn (19) to yield

$$\dot{\tau}_d = \frac{1}{K_\tau}(M\ddot{\omega}_d + B\dot{\hat{\omega}} + k_s\dot{e} + k_{N1}k_0^2\dot{e}), \tag{29}$$

which can be substituted into Eqn (28) to yield

$$\dot{\eta} = \frac{1}{K_\tau}(M\ddot{\omega}_d + B\dot{\hat{\omega}} + k_s\dot{e} + k_{N1}k_0^2\dot{e}) + RI\Omega_4 + K_B\omega g(I)\Omega_4 - \Omega_4 v. \tag{30}$$

The dynamics of the velocity estimation error $\dot{\tilde{\omega}}$ in Eqn (13) are substituted in Eqn (30) to yield

$$\dot{\eta} = \frac{1}{K_\tau}\left(M\ddot{\omega}_d + \frac{B}{M}(k_0\tilde{\omega} - B\hat{\omega} - T_L + K_\tau Ig(I)) + k_s\dot{e} + k_{N1}k_0^2\dot{e}\right) + RI\Omega_4 + K_B\omega g(I)\Omega_4 - \Omega_4 v. \tag{31}$$

Substitutions are now made for $\dot{e}$ from Eqn (22) and the result is then simplified using $\Omega_1$, $\Omega_2$, and $\Omega_3$ defined in Eqn (17) to yield

$$\dot{\eta} = \Omega_1 + \Omega_2\omega + \Omega_3\tilde{\omega} - \Omega_4 v. \tag{32}$$

Substitution of the input control voltage $v$ from Eqn (16) yields the closed-loop torque tracking error dynamics in the form

$$\dot{\eta} = (\Omega_2 + \Omega_3)\tilde{\omega} - k_{N2}(\Omega_2 + \Omega_3)^2\eta - K_\tau e - k_s\eta. \tag{33}$$

After substitutions for $\dot{V}_0(t)$ from Eqn (15) and from the two error systems in Eqns (24) and (33) into Eqn (21), we obtain the following upper bound for $\dot{V}(t)$:

$$\begin{aligned}\dot{V} \leq & -k_0\tilde{\omega}^2 - k_s e^2 + [-k_0\tilde{\omega}e - k_{N1}k_0^2 e^2] \\ & + [(\Omega_2 + \Omega_3)\tilde{\omega}\eta - k_{N2}(\Omega_2 + \Omega_3)^2\eta^2] - k_s\eta^2.\end{aligned} \tag{34}$$

As described in [20], the nonlinear damping argument can be used to bound the bracketed pairs of terms in Eqn (34) to produce

$$\dot{V} \leq -k_0\tilde{\omega}^2 - k_s e^2 + \frac{\tilde{\omega}^2}{k_{N1}} + \frac{\tilde{\omega}^2}{k_{N2}} - k_s\eta^2. \tag{35}$$

A new upper bound for $\dot{V}(t)$ is found by defining $k_N = k_0 - 1/k_{N1} - 1/k_{N2} > 0$ in order to write

$$\dot{V} \leq -k_N\tilde{\omega}^2 - k_s e^2 - k_s\eta^2. \tag{36}$$

Therefore, $\dot{V}(t)$ is negative definite if the control gains are restricted by

$$k_0 > \frac{1}{k_{N1}} + \frac{1}{k_{N2}}. \tag{37}$$

**Remark 4.1.** The usefulness of the Lyapunov-like analysis as a guide in the control design can be seen in Eqns (20) and (36) where it would typically be concluded that the controller causes the rotor velocity to approach the desired velocity exponentially fast. However, we are prevented from drawing such conclusions by the facts that the condition $I = 0$ may disrupt the controller and more importantly the desired torque may be physically unrealizable. The filters in Remark 3.1 and section 4.1 allow the

controller to be implemented but it is not obvious how this modification can be incorporated into a general stability result.

## 5. EXPERIMENTAL RESULTS

The proposed observer and controller were used to control the velocity of an industrial motor. This section describes the experimental setup shown in Fig. 2, the motor under test, and the results of the velocity control experiment. The mechatronics testbed used to implement the controller consists of the following hardware: (1) an Intel 486 based PC, (2) a TMS320C30 DSP system board from Spectrum Signal Processing, (3) a Techron 7570 linear amplifier, (4) a Hall effect current sensor, (5) a BEI Motion Systems Co. 1000-line encoder (used only for validation of the controller performance), (6) a Himmelstein torque transducer (used only to develop a flux saturation model), and (7) assorted interfacing electronics. The proposed observer/controller is compiled in C code according to the block diagram in Fig. 1 and is executed on the DSP board. At fixed sample times a voltage control signal is generated by the DSP board according to the control algorithm and the measured current; this signal is then applied to the motor through the linear power amplifier. Although the sample period is small (500 $\mu$sec), it is to be expected that the implementation of the inherently analog observer/controller in a digital fashion will lead to quantization error. However, this affect appears to be limited as seen in the final velocity tracking results. In the testbed, the PC simply provides an interface between the user and the DSP board.

The Baldor CD3433, 1/3 hp wound stator D.C. motor connected in a series configuration was used in the experiment. The electromechanical system parameters for the motor model in Eqns (1) through (3) were determined to be

$$M = 0.035\ \text{kg} \cdot \text{m}^2, \qquad B = 0.009\ \text{N} \cdot \text{m/s}, \qquad K_\tau = 0.415\ \text{N} \cdot \text{m/Wb} - \text{A}$$

$$R = 62.25\ \Omega, \qquad K_B = 0.415\ \text{V} \cdot \text{s/Wb}.$$

The saturation function, $g(I)$, was determined with the motor in a separately excited configuration as follows. The motor was mechanically connected to an inertial load via a torque sensor, S. Himmelstein and Company Model MCRT 2801T. The inertial

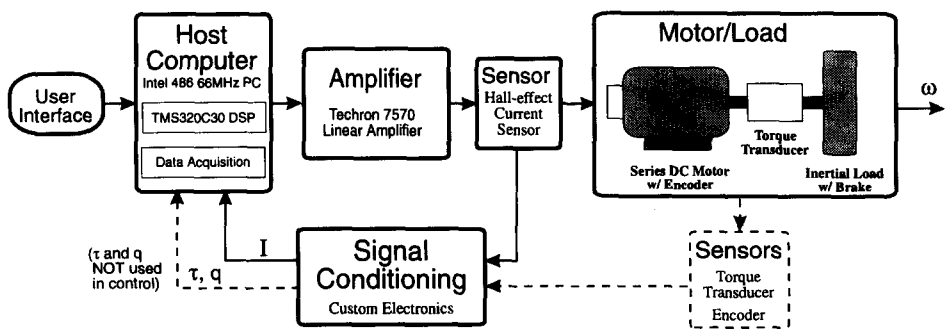


Fig. 2. Mechatronics testbed.

load was braked using a band-type friction brake set to create a small load torque. Data points were obtained for the left-hand side of Eqn (2) by applying constant stator and rotor voltages in order to produce a constant rotor torque. Based on the current readings, the measured torque, and the known value of $K_T$ the plot of $g(I)$ shown in Fig. 3 was obtained. The resemblance of the curve to the arctan $(\cdot)$ function motivated the use of this function to match the recorded behavior and to meet the strictly increasing and differentiability requirements. The final form of $g(I)$ was determined to be

$$g(I) = 0.941 \arctan(2.6I)\text{Wb},$$

from which $f(I)$ of Eqn (6) is determined to be

$$f(I) = \ln(\arctan(2.6I)).$$

With the electromechanical model completely specified, the velocity tracking experiment was performed. The motor was mechanically connected to an inertial load, an iron wheel attached directly to the rotor shaft (for the tracking experiment no external load was added, i.e. $T_L = 0$). A desired trajectory for the rotor position was specified as

$$\omega_d(t) = \begin{cases} 1146\,(1 - e^{-0.001t^3})\,\text{deg/s} & 0 \leq t < 25 \\ 1146\,(1 - e^{-0.001t^3}) + 573\,(1 - e^{-0.001(t-25)^3})\,\text{deg/s} & 25 \leq t \end{cases}$$

which has the desirable property $\omega_d(0) = \dot{\omega}_d(0) = \ddot{\omega}_d(0) = 0$. It is important to note that $\omega_d(t)$, $\dot{\omega}_d(t)$, and $\ddot{\omega}_d(t)$ are continuous. The initial conditions for all of the state variables were set to *zero*. After some experimentation, we achieved the best velocity

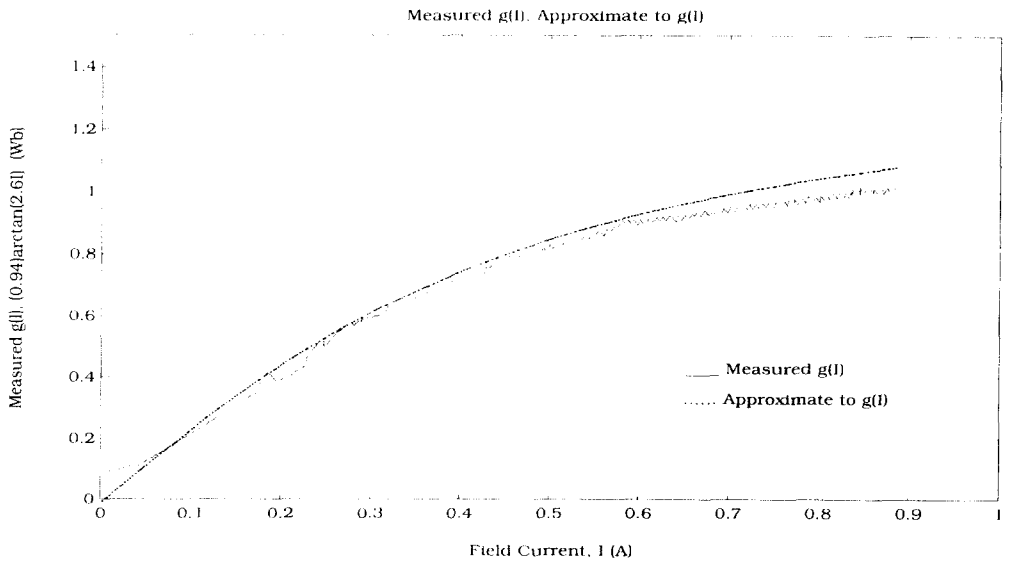


Fig. 3. Measured and approximated saturation function.

tracking with the control gains set to

$$k_{N1} = 0.8, \quad k_{N2} = 0.02, \quad k_0 = 0.034, \quad k_s = 0.113$$

and the filter in Eqn (9) was used on $I$ with $\alpha = 0.1$ to prevent division by *zero*.

The results of the experiment are summarized in Figs 4 through 7. The plot in Fig. 4 shows the actual and desired velocities and provides the basis for concluding

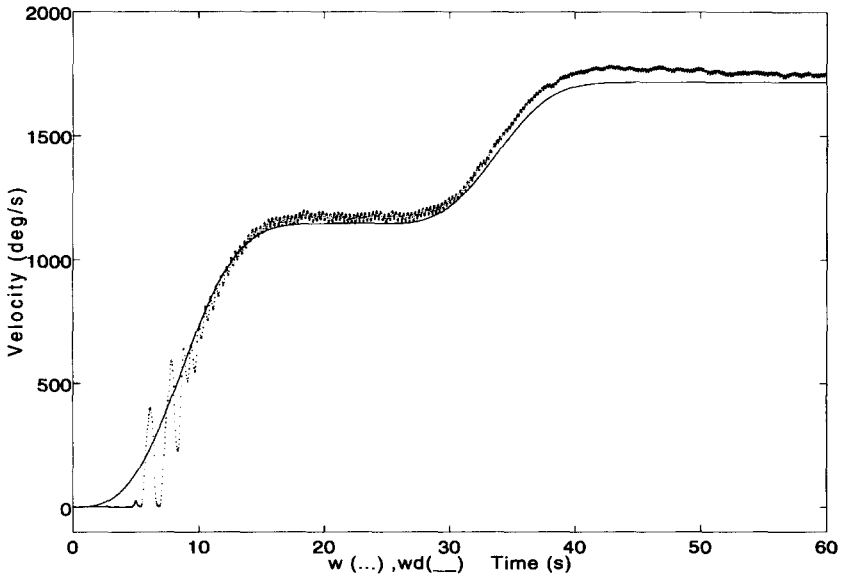


Fig. 4. Measured and desired velocities.

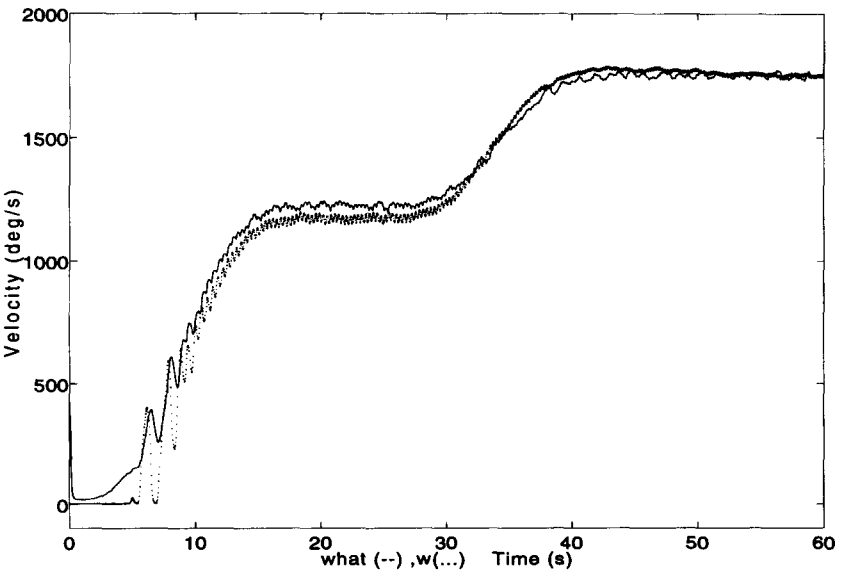


Fig. 5. Measured and estimated velocities.

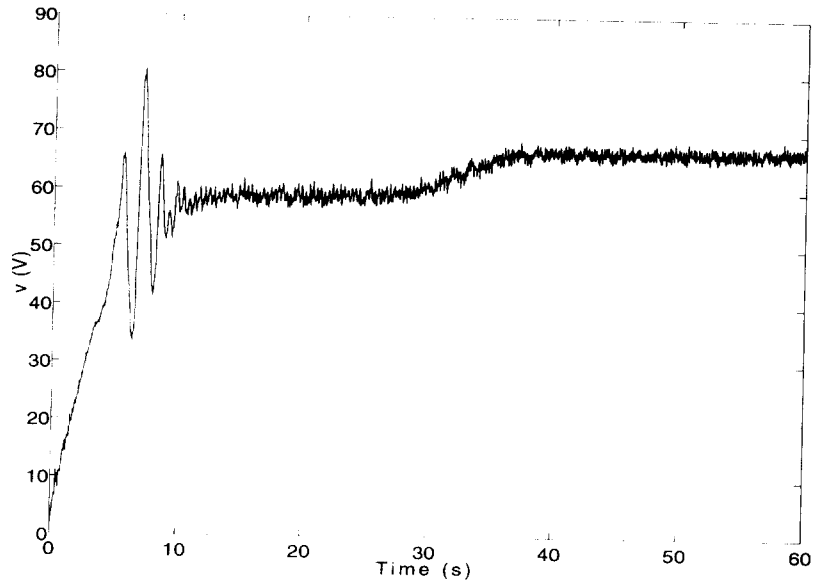


Fig. 6. Input voltage.

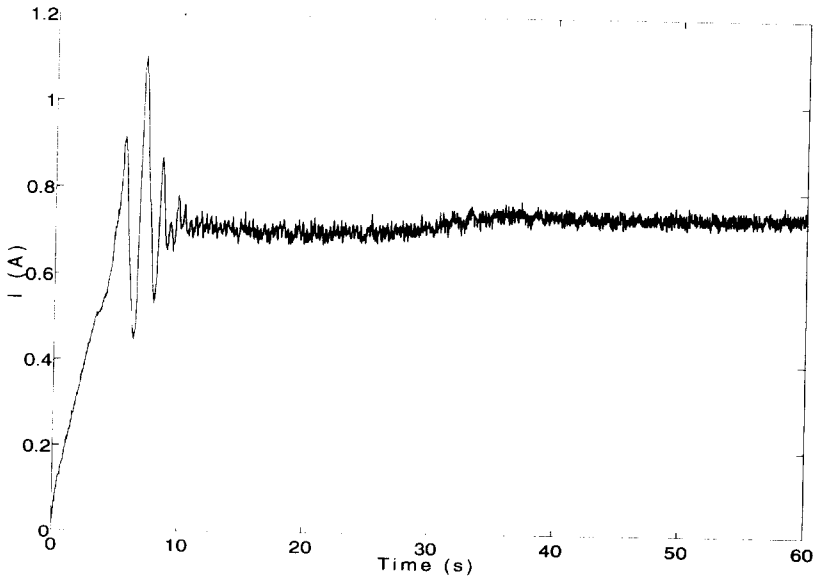


Fig. 7. Current.

that the control system is functioning as desired. The actual velocity was obtained using a backward difference algorithm on the position signal (it must be emphasized that the encoder was used as part of the experimental validation but was not used in the controller or observer implementation). Note that due to measurement noise, modeling error, quantization error, in applying the control, and use of the various

filters to patch the control, the tracking error does not approach zero. The velocity estimate is compared to the actual velocity in Fig. 5. Figure 6 plots the input voltage, and Fig. 7 shows the resulting current.

**Remark 5.1.** The condition on the control gains in Eqn (37) was not satisfied in the selection of the control gains as it turned out to be overly conservative and hindered fine tuning of the controller performance. It should be reiterated that the Lyapunov-like analysis provided the framework for designing the observer/controller system. That is, each of the terms in both the observer and controller are specified to facilitate this analysis. The fact that the gain selection criteria are not fulfilled would suggest that although the Lyapunov-like analysis has dictated the structure of the controller, the use of certain terms has been overstated, i.e. that some control gains are required to be unnecessarily large in this analysis.

**Remark 5.2.** The external load torque used in this experiment was set to *zero* due to the physical construction of the motor. The CD3433 motor is listed in the Baldor catalog for use in shunt connection and has maximum current ratings of 3.7 and 0.4 A for the armature and field currents, respectively. This same motor rewired in a series connection for use in this experiment has a maximum current rating set by the smaller of the field and armature ratings. Thus, in this experiment we have a physically large motor, i.e. large rotor inertia and mechanical dampening, that can only produce a small torque. In this system the friction of the motor and the connected load will allow for only a small load torque. Note that, in general, a motor that is specifically constructed for use in a series connection must always be connected to a load torque in order to prevent speed run-away [1].

## 6. CONCLUSIONS

Through the observed integrator backstepping technique we have formulated a controller to achieve velocity tracking control for the series connected D.C. motor. The stability result typically associated with this design technique is forfeited when the basic controller of [18] is modified to reflect the unidirectional torque production capability of the motor and the limitations associated with observing the rotor velocity from the electrical dynamics. The results of a velocity tracking experiment are offered as validation that the proposed controller does in fact produce velocity tracking.

*Acknowledgements*—This work is supported in part by the U.S. National Science Foundation Grants DDM-931133269, DMI-9457967, DOE Contract DE-AC21-92MC29115, the Office of Naval Research Grant URI-3139-YIP01, and the Union Camp Corporation.

## REFERENCES

1. Chiasson J., Nonlinear differential-geometric techniques for control of a series DC motor. *IEEE Trans. Control Syst. Technol.* **2**(1), 35–42 (1994).
2. Harashima F., Hashimoto H. and Kondo S., MOSFET converter-fed position servo system with sliding mode control. *IEEE Trans. Ind. Elect.* **IE-32**(4), Aug. (1985).

3. Dote Y. and Hoft R., Microprocessor based sliding mode controller for DC motor drives. *IEEE/IAS Conf. Rec.*, pp. 641–645 (1980).
4. Brickwedde A., Microprocessor-based adaptive speed and position regulation for electrical drives. *IEEE Trans. Ind. Applic.* **IA-21**(5), 1154–1161 (1985).
5. Olivier P., Feedback linearization of DC motors. *IEEE Trans. Ind. Elect.* **38**(6), 498–501 (1991).
6. Chiasson J. and Bodson M., Nonlinear control of a shunt DC motor. *IEEE Trans. Aut. Control* **38**(11), 1662–1666 (1993).
7. Bodson M., Chiasson J., Novotnak R. and Rekowski R., High-performance nonlinear feedback control of a permanent magnet stepper motor. *IEEE Trans. Control Syst. Technol.* **1**(1), 5–14 (1993).
8. Canudas C., Ortega R. and Seleme S., Robot motion control using induction motor drives. *Proc. 1993 IEEE Int. Conf. Robotics and Automation*, Vol. 2, pp. 533–538, Atlanta, GA, June (1993).
9. Carroll J., Dawson D. and Qu Z., Adaptive tracking control of a switched reluctance motor turning an inertial load. *Proc. Am. Control Conf.*, pp. 670–674, San Francisco, CA, June (1993).
10. Carroll J. and Dawson D., Robust tracking control of a BLDC motor with application to robotics. *Proc. 1993 IEEE Int. Conf. Robotics and Automation*, Vol. 1, pp. 94–99, Atlanta, GA, June (1993).
11. Chen D. and Paden B., Adaptive linearization of hybrid step motors: stability analysis. *IEEE Trans. Aut. Control* **38**(6), 874–887 (1993).
12. Hemati N., Thorp J. and Leu M., Robust nonlinear control of brushless DC motors for direct-drive robotic applications. *IEEE Trans. Ind. Elect.* **37**(6), 498–501 (1990).
13. Kanellakopoulos I., Krein P. and Disilvestro F., A new controller-observer design for induction motor control. *Proc. of the ASME Winter Meeting*, DSC Vol. 43, pp. 43–47, Anaheim, CA, December (1992).
14. Marino R., Peresada S. and Valigi P., Adaptive partial feedback linearization of induction motors. *Proc. IEEE Conf. Decision and Control*, pp. 3313–3318, Brighton, U.K., December (1991).
15. Taylor D., Adaptive control design for a class of doubly-salient motors. *Proc. IEEE Conf. Decision and Control* Vol. 3, pp. 2903–2908, Brighton, U.K., December (1991).
16. Bass J., Ehsani M. and Miller T., Simplified electronics for torque control of sensorless switched-reluctance motor. *IEEE Trans. Ind. Elect.* **IE-34**(2), 234–239 (1987).
17. Meshkat S. and Tessarolo A., Part II: sensorless brushless DC motor control using DSPs and Kalman filtering. *Power Conversion Intell. Motion* **Aug.**, 45–50 (1993).
18. Burg T., Dawson D., Hu J. and Vedagarbha P., Velocity tracking control for a separately excited DC motor without velocity measurements. *Proc. 1994 American Control Conf.*, pp. 1051–1056, Baltimore, MD, June (1994).
19. Kokotovic P., The joy of feedback: nonlinear and adaptive. *IEEE Contr. Syst. Mag.* **12**, 7–17 (1992).
20. Kanellakopoulos I., Adaptive control of nonlinear systems. Ph.D. dissertation, University of Illinois, Urbana, IL (1992).